Received: 12 June 2017 | Accepted: 17 July 2017

DOI: 10.1111/gcb.13874

PRIMARY RESEARCH ARTICLE

WILEY Global Change Biology

Assessment of ecosystem resilience to hydroclimatic disturbances in India

Ashutosh Sharma | Manish Kumar Goyal

Department of Civil Engineering, Indian Institute of Technology Guwahati, Guwahati, India

Correspondence
Manish Kumar Goyal, Department of Civil Engineering, Indian Institute of Technology Guwahati, Guwahati, India.
Email: mkgoyal@iitg.ernet.in

Abstract

Recent studies have shown an increasing trend in hydroclimatic disturbances like droughts, which are anticipated to become more frequent and intense under global warming and climate change. Droughts adversely affect the vegetation growth and crop yield, which enhances the risks to food security for a country like India with over 1.2 billion people to feed. Here, we compared the response of terrestrial net primary productivity (NPP) to hydroclimatic disturbances in India at different scales (i.e., at river basins, land covers, and climate types) to examine the ecosystems' resilience to such adverse conditions. The ecosystem water use efficiency *(WUE_e: NPP/ Evapotranspiration)* is an effective indicator of ecosystem productivity, linking carbon (C) and water cycles. We found a significant difference ($p < .05$) in WUE_e across India at different scales. The ecosystem resilience analysis indicated that most of the river basins were not resilient enough to hydroclimatic disturbances. Drastic reduction in WUE_e under dry conditions was observed for some basins, which highlighted the cross-biome incapability to withstand such conditions. The ecosystem resilience at land cover and climate type scale did not completely relate to the basin-scale ecosystem resilience, which indicated that ecosystem resilience at basin scale is controlled by some other ecohydrological processes. Our results facilitate the identification of the most sensitive regions in the country for ecosystem management and climate policy making, and highlight the need for taking sufficient adaptation measures to ensure sustainability of ecosystems.

KEYWORDS

climate change, droughts, ecosystem resilience, evapotranspiration, net primary productivity, water use efficiency

1 | INTRODUCTION

As per Intergovernmental Panel on Climate Change (IPCC), the global surface temperature will rise and precipitation regimes around the globe will change substantially under climate change in the 21st century (Pachauri & Meyer, 2014). However, the impacts of climate change are not limited to the atmosphere or hydrosphere, but it also has a profound influence on ecosystem functioning (Dale, Joyce, McNulty, & Neilson, 2000; Karl & Trenberth, 2014; Meehl & Tebaldi, 2004; Wheeler & Von Braun, 2013). The productivity of terrestrial ecosystems is adversely affected by the hydroclimatic disturbances such as droughts (Breshears et al., 2005; Dale et al., 2000; Thomey et al., 2011; Xu et al., 2017; Zhao & Running, 2010), which have implications for the food security, especially for a country like India with a population over 1.2 billion (Zhang, Obringer, Wei, Chen, & Niyogi, 2017). Terrestrial ecosystems also play an important role in global carbon cycle as a major sink for atmospheric CO_2 (Cao & Woodward, 1998; Ciais, Tans, Trolier, White, & Francey, 1995; Yu et al., 2014). Terrestrial plants take out CO_2 from the atmosphere through photosynthesis along with the loss of water, which regulates the mass-energy exchange between the vegetation and the atmosphere (Keenan et al., 2013). The terrestrial net primary production (NPP) is defined as the difference between the plant photosynthesis and the autotrophic respiration (Roxburgh, Berry, Buckley, Barnes, & Roderick, 2005). NPP is an effective indicator for ecosystem functioning and carbon fluxes from ecological and physiological processes (Cao & Woodward, 1998). Climatic conditions such as precipitation, temperature, and solar radiation control the primary productivity (Running et al., 2004). The increase in NPP during 1982-1999 was attributed to the eased critical climatic constraints on plant growth (Nemani et al., 2003). Water stress is one of the most important limiting factors, which directly or indirectly constrains the vegetation productivity (Mu, Zhao, & Running, 2011a). The water loss from the ecosystem can be divided into two parts: (i) "physiologically productive water" which represents the transpiration during the growing season, and (ii) "nonproductive" water loss which includes the water loss from canopy interception and evaporation from bare soil (Sun et al., 2016). These two parts of ecosystem water use are controlled differently by the climatic factors. The reduction in NPP during 2000–2009 was attributed to the large-scale droughts, which indicated the importance of water as limiting factor for the vegetation productivity (Zhao & Running, 2010). In Europe, the reduction in gross primary productivity was attributed to the rainfall deficit and extreme summer heat in 2003 (Ciais et al., 2005). Hence, water stress or drought has a significant impact of terrestrial ecosystems as a constraint on vegetation growth. The ecosystem water use efficiency (WUE_e), defined as the ratio of the rate of carbon uptake and the water loss, indicates the interaction of carbon and water fluxes between the terrestrial ecosystem and atmosphere (Jones, 2004; Niu et al., 2011; Song et al., 2017; Tang et al., 2014). It is one of the most important factor controlling plant productivity in dry environments (Mu et al., 2011a). The hydroclimatic conditions play a crucial role in spatiotemporal variation in WUE_e by affecting the ecosystem evaporation, transpiration, and carbon uptake (Niu et al., 2011; Yang et al., 2016).

The spatiotemporal pattern of WUE_e and its environmental controls play an important role in understanding the responses of terrestrial ecosystems to climate change. Several global and regional studies have been carried out around the globe, but there are very few studies in India (Huang et al., 2015, 2016; Song et al., 2017; Tang et al., 2014). The quantification of the patterns of WUE_e is needed to assess the natural and human impacts on terrestrial ecosystems in the country. A better understanding of how WUE_e responds to hydroclimatic changes will provide insight into how carbon and water cycles will change under hydroclimatic alterations caused due to global climate change (Huang et al., 2015).

In this work, we compared the functional response of WUE_e to hydroclimatic disturbances (particularly droughts) to examine the ecosystem resilience, which is defined as the ability of the ecosystem to absorb the disturbances and sustain the same functioning under disturbed conditions (Ponce Campos et al., 2013; Walker, Holling, Carpenter, & Kinzig, 2004). The climate in most parts of India is tropical or temperate and hence, the vegetation productivity is controlled by the water/precipitation (Running et al., 2004; Sun et al., 2016). However, an increase in both drought severity and frequency has been reported both globally (Dai, 2011, 2013) and in India (Mallya, Mishra, Niyogi, Tripathi, & Govindaraju, 2015). In addition, droughts in India have shifted toward the agriculturally important Indo-Gangetic, central Maharashtra, and coastal south-India plains in recent past (Mallya et al., 2015), which adds to the risk for food security in future as it has already been a serious concern due to overexploited groundwater (Asoka, Gleeson, Wada, & Mishra, 2017) and fluctuating monsoon rainfall (Mallya et al., 2015). Hence, in this study, we have tried to assess the impact of water-limited conditions on the NPP and WUE_e.

During the early twenty-first century drought, the ecosystems in North America and Australia showed remarkable cross-biome resilience, which was assessed using WUE_e by Ponce Campos et al. (2013). A resilient ecosystem absorbs the disturbances and sustains its productivity by increasing or maintaining WUE_e under water-limited conditions induced by lesser annual precipitation, whereas a nonresilient ecosystem is not able to sustain productivity under such conditions. We carried out ecosystem resilience assessment at river basin scale for better representation of hydroclimatic disturbances, considering 22 major river basins in India as defined by India-WRIS (India-WRIS, 2014). We used satellite datasets, terrestrial NPP product (MOD17A3), and Evapotranspiration product (MOD16A3) from the Moderate Resolution Imaging Spectroradiometer (MODIS), for spatiotemporal assessment of WUE_e over 2000 to 2014. The satellites datasets were used due to the unavailability of eddy covariance sites in India. These satellite products have been used in many regional and global studies (Anav et al., 2015; Turner et al., 2006; Xue, Guo, Otto, Xiao, & Tao, 2015; Zhao & Running, 2010). The comparative assessment of different river basins is important for helping to understand how future climate change will affect the carbon and energy budgets in different regions. However, the diversity of responses to disturbances among different ecosystem components plays an important role in defining the overall ecosystem resilience (Elmqvist et al., 2003) and hence, the assessment of the contribution of different factors is necessary. Therefore, the basin-scale assessment of WUE_e or ecosystem resilience was further related to land cover and climate types to understand the role of these factors. The objectives of this study were to compute and relate the WUE_e at different scales (river basin, land cover, and climate type) in India and to evaluate the ecosystem resilience of different river basins in India and its relation with the ecosystem resilience at land cover and climate type scales.

2 | MATERIALS AND METHODS

2.1 | River basin definition

For this study, river basins in India were defined as per the India-WRIS (Water Resources Information System) report "Watershed

Atlas of India" (India-WRIS, 2014). The study was carried out at 22 river basins (Fig. S1, Table S1). Table S1 shows the watershed details and mean annual precipitation (MAP, mm/year) for different basins. Fig. S1 shows the location of basins and the spatial distribution of precipitation in India. Ganga Basin (*Basin Id 2a*) is the largest basin in terms of the geographical area (8,61,452 km^2), whereas East flowing rivers between Godavari and Krishna Basin (*Basin Id 16*) is the smallest basin (12,289 km^2). West flowing rivers South of Tapi Basin (*Basin Id 14*) receive the highest mean annual rainfall amount of 2755 mm/year due to the presence of Western Ghats. West flowing rivers of Kutch and Saurashtra including Luni Basin (*Basin Id 20*), which covers the arid and semi-arid regions of Rajasthan and Gujarat, receive the least mean annual rainfall amount of 560 mm/year.

2.2 | MODIS NPP

We used the global annual MOD17A3 products (Version: 055) from the NASA Earth Observation System (EOS) program. The global dataset was developed by Numerical Terradynamic Simulation Group (NTSG) at University of Montana (UMT) (available from http://www.ntsg.umt.edu/project/mod17). The MOD17A3 product was generated using the MOD17 algorithm (Running et al., 2004; Zhao, Heinsch, Nemani, & Running, 2005). The global MODIS NPP and Gross Primary Productivity (GPP) products showed no overall bias across multiple biomes (Turner et al., 2006). The MOD17A3 product has been validated and used in many studies (Turner et al., 2006; Zhao, Running, & Nemani, 2006; Zhao et al., 2005). We used annual NPP dataset from 2000 to 2014 at a spatial resolution of 1 km. There is a significant spatial variation in mean annual MODIS NPP across India (Fig. S2). Northeastern and Western Ghats regions have higher mean annual NPP (>1500 gC/m^2), whereas the arid regions of western India have the least NPP.

2.3 | MODIS ET

We used evapotranspiration data from the global annual MOD16A3 product from the NASA Earth Observation System (EOS) program. The dataset is available at same resolution from 2000 to 2014 (available from http://ntsg.umt.edu/project/mod16). The MOD16 ET datasets were estimated using improved ET algorithm (Mu, Heinsch, Zhao, & Running, 2007; Mu, Zhao, & Running, 2011b, 2013). Like NPP, there is substantial variation in mean annual ET across India (Fig. S3).

2.4 | Koppen-Geiger climate classification

The Koppen-Geiger climate classification maps were prepared based on recent datasets from the Climatic Research Unit (CRU) of the University of East Anglia and the Global Precipitation Climatology Centre (GPCC) at the German Weather Service (Kottek, Grieser, Beck, Rudolf, & Rubel, 2006; Rubel & Kottek, 2010) (available from: http://koeppen-geiger.vu-wien.ac.at/present.htm).

2.5 | Meteorological data

We obtained the daily gridded rainfall dataset (IMD4) from Indian Meteorological Department (IMD) at a high spatial resolution ($0.25° \times 0.25°$) which provides data over the Indian mainland (Pai et al., 2014). The data were prepared from daily rainfall records from 6955 rain gauge stations in India and is available from 1901 to 2015. The total annual precipitation (sum of daily precipitation, mm/year) and mean annual precipitation (mean of annual precipitation, mm/year) at same resolution were computed from daily values.

2.6 | Ecosystem water use efficiency *(WUE_e)*

The annual WUE_e was computed at pixel level using annual rasters of MODIS NPP and ET. First, the pixels corresponding to the valid and nonfill values of NPP and ET were identified and, then, WUE_e was computed for every valid pixel to represent its spatial variations within a basin. The average WUE_e was computed as the average for all pixels. The mean annual WUE_e (denoted as WUE_m) over 15 years (2000–2014) was computed by averaging all rasters.

2.7 | Ecosystem resilience analysis

The WUE_e during the driest year, denoted as WUE_d, in the study duration was compared with the WUE_m for each basin to examine the ecosystem resilience. As water is the climatic control for NPP over India (see Figure 1 of Running et al. 2004), the hydroclimatic disturbances were identified based on annual precipitation. The driest year was chosen based on the annual precipitation and Standardized Precipitation Index (SPI) and Standardized Precipitation Evapotranspiration Index (SPEI) (McKee, Doesken, & Kleist, 1993; Vicente-Serrano, Beguería, & López-Moreno, 2010). SPI for the period 2000–2014 was computed based on long-term precipitation series (1901–2015), whereas the SPEI was computed based on long-term precipitation and temperature series (1951–2014) from IMD. The negative values of SPI represent the dry conditions. As the productivity of resilient ecosystems should not be affected by the disturbance (i.e., the water-limited conditions), the ecosystem that sustains its productivity by increasing or maintaining its WUE_m during the driest year was considered as resilient. We defined an index R_d (Equation 1) that represents the ratio of WUE_d and WUE_m.

$$R_d = \frac{WUE_d}{WUE_m} \tag{1}$$

The dimensionless R_d can be used for comparative assessment of ecosystem resilience of different basins. Different classes were formed based on the value of R_d. If R_d is greater than or equal to 1, the ecosystem is resilient to disturbances as it sustained its productivity despite the disturbed conditions by increasing the WUE_e. If R_d lies between 0.9 and 1, the basin is termed as slightly nonresilient, as the productivity of the basin is not much affected by the disturbances. If R_d is between 0.8 and 0.9, the basin is termed as moderately nonresilient and if R_d is less than 0.8, the basin is termed as severely nonresilient.

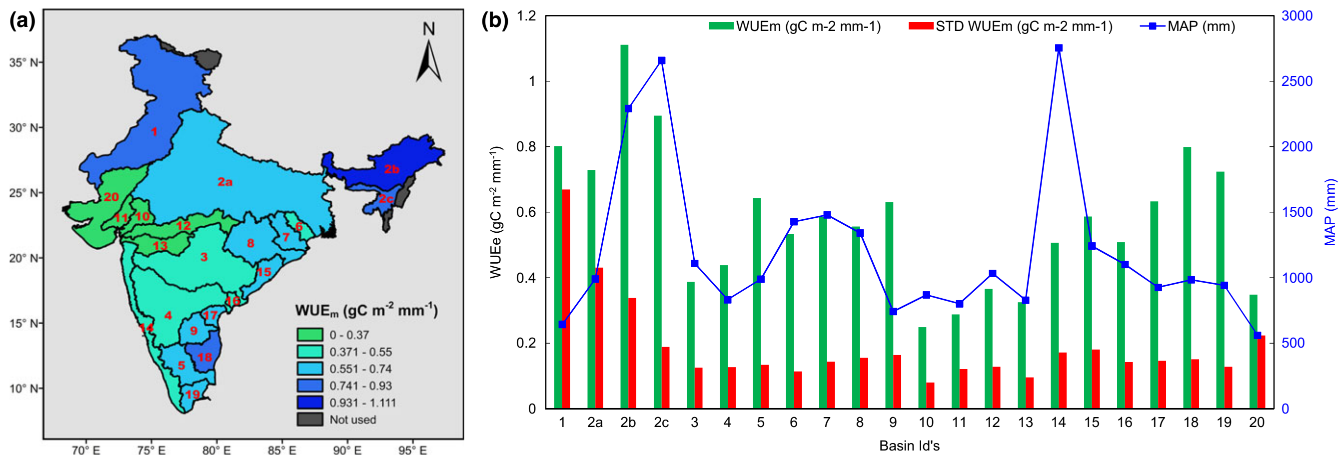

FIGURE 1 Mean annual ecosystem water use efficiency (WUE_e = NPP/ET) across different basins in India over 2000–2014. Spatial distribution of WUE_m across basins (a) and variation in mean and standard deviation (STD) of WUE_m (b). MAP is the mean annual precipitation (mm/year) of the basin

3 | RESULTS

3.1 | Basin-scale WUE_e

The mean annual WUE_e (denoted as WUE_m) showed considerable spatial variations over India due to different climate, soils, and vegetation types. Figure 1a,b show the WUE_m and standard deviation (STD) for different river basins in India. There was a significant difference, F (21,308) = 127.35, $p < .01$ (ANOVA), in WUE_m across basins. The basins in the northeastern parts of the country had higher WUE_m followed by northern, eastern, southern, and western regions, respectively (Figure 1a). The spatial variation in WUE_m is closely related to the variations in the mean annual precipitation (see Fig. S1) and NPP (see Fig. S2). WUE_e for Brahmaputra basin (Basin Id. 2b, WUE_m = 1.111 gC m^{-2} mm^{-1}) in the northeastern regions was significantly higher ($p < .01$) than for other basins, whereas Mahi basin (Basin Id. 10) in the western region had the least WUE_m (= 0.249 gC m^{-2} mm^{-1}). The standard deviation (STD, Figure 1b) of the pixel values of WUE_m was highest for Indus basin (Basin Id 1), followed by Ganga (Basin Id 2a) and Brahmaputra basins (Basin Id 2b), respectively, due to larger geographical areas and presence of different climate and vegetation types in the basins. STD was less than 0.2 gC m^{-2} mm^{-1} for all other basins, indicating lesser spatial variations within the basins.

3.2 | Land-cover-scale WUE_e

Different vegetation types differ in carbon uptake and water consumption, leading to the differences in WUE_e. Figure 2a shows the spatial distribution of different land cover types in India. This land cover classification is based on 10 years (2001–2010) of Collection 5.1 MCD12Q1 land cover type data and was obtained from the USGS Land Cover Institute (LCI, https://landcover.usgs.gov/global_climatology.php) (Broxton, Zeng, Sulla-Menashe, & Troch, 2014). Croplands (CR) is the most dominant land cover type in India, covering about 50% of the total geographical area. Figure 2b shows the WUE_m for major land cover types. It can be seen that forest classes had higher WUE_m compared to other vegetation types, which is consistent with the global studies (Tang et al., 2014). The highest WUE_m (= 1.087 gC m^{-2} mm^{-1}) was found for Mixed Forests (MF), followed by Deciduous Needleleaf Forest (DNF, WUE_m = 1.001 gC m^{-2} mm^{-1}), Evergreen Needleleaf Forest (ENF, WUE_m = 0.959 gC m^{-2} mm^{-1}), and Evergreen Broadleaf Forest (EBF, WUE_m = 0.948 gC m^{-2} mm^{-1}). In contrast to other forest types, Deciduous Broadleaf Forest (DBF) had much smaller WUE_m (= 0.416 gC m^{-2} mm^{-1}), however, DBF accounts for only 0.56% area. All nonforest land covers had WUE_m less than 0.7 gC m^{-2} mm^{-1}.

3.3 | Climate type scale WUE_e

India has a diverse spatial distribution of different climate types (Peel, Finlayson, & McMahon, 2007). Figure 3a shows the spatial distribution of Koppen-Geiger climate classes in India, which was derived from Kottek et al. (2006). Southern parts of the country have tropical (A) climate, northwestern parts have dry (B) climate, northern and northeastern parts have temperate climate (C), and Himalayan parts have polar climate (E). Of 31 different climate types identified in India by Kottek et al. (2006), we considered the climate types having spatial coverage of more than 2.5% of the total geographical area. Temperate climate types, *Cwa* and *Cwb*, had highest WUE_m of 1.055 gC m^{-2} mm^{-1} and 1.009 gC m^{-2} mm^{-1}, respectively, followed by equatorial and arid climates (Figure 3b), which was consistent with global studies (Xia, Wang, Mu, Jin, & Sun, 2015). Arid climates, *BWh* and *BSh*, had least WUE_m of 0.175 gC m^{-2} mm^{-1} and 0.475 gC m^{-2} mm^{-1}, respectively.

3.4 | Ecosystem resilience analysis at river basin scale

Table 1 shows the results of the ecosystem resilience analysis of different river basins. The table shows the computation of R_d, which indicates the degree to which an ecosystem is affected by

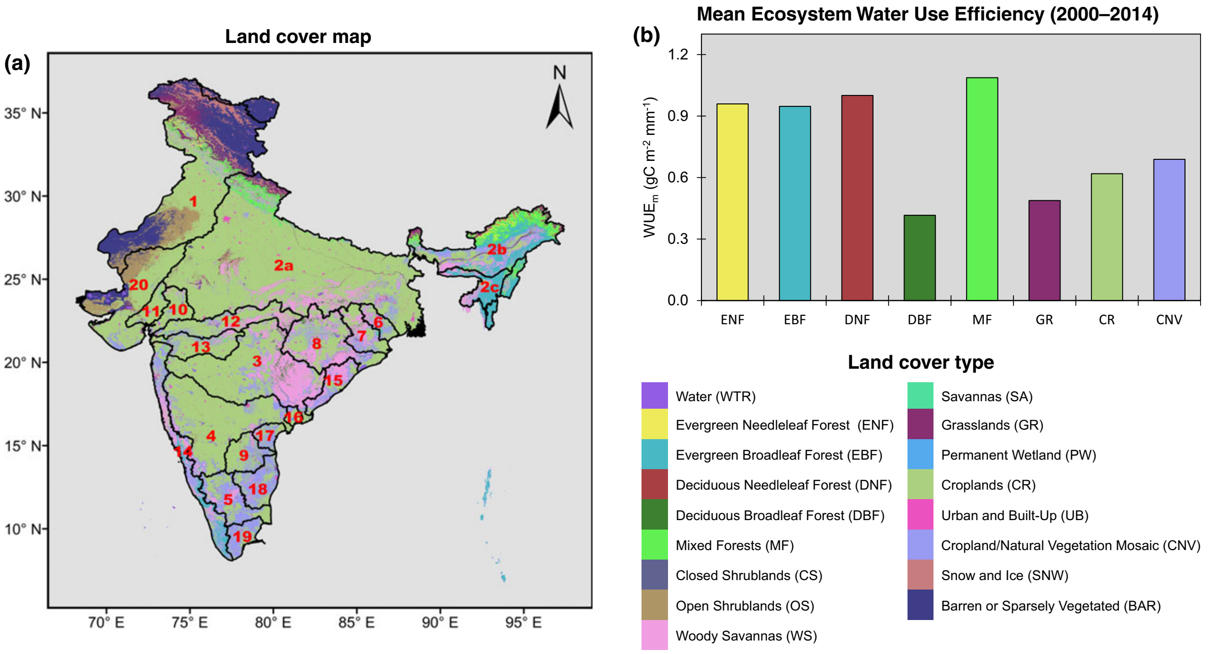

FIGURE 2 Spatial distribution (a) and mean annual ecosystem water use efficiency (WUE_m) (b) of different land cover types in India. Annual ecosystem water use efficiency ($WUE_e = NPP/ET$) was computed using MODIS NPP and ET products over 2000–2014

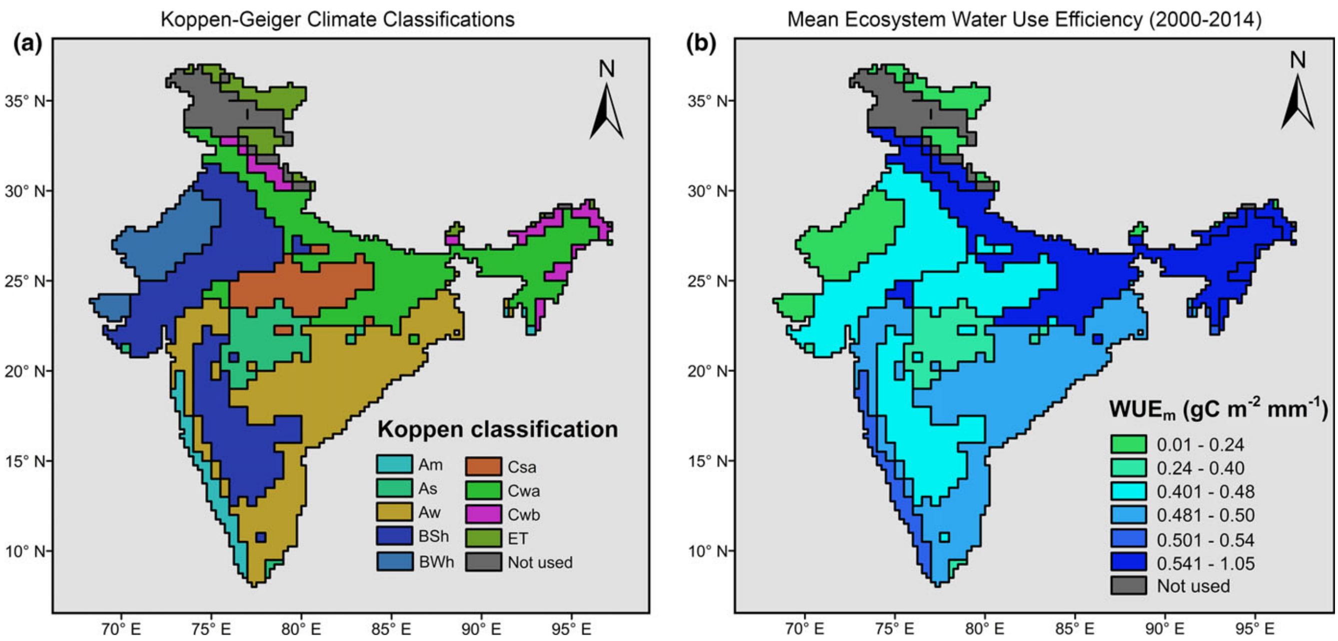

FIGURE 3 Spatial distribution of Koppen-Geiger climate types (a) and the corresponding mean annual ecosystem water use efficiency (WUE_m) (b). Climate classes with an area less than 2.5% of total area were not used in this study

the hydroclimatic disturbances. Higher the value of R_d, higher the resilience of ecosystem. Our results showed that only 6 basins (*Basin Id's 1, 2b, 9, 17, 18, and 20*) of 22 river basins were resilient to climatic disturbances in the study duration (Figure 4). Indus basin (*Basin Id. 1*) had the highest R_d, which indicated that the ecosystems in this basin sustained their productivity by increasing the WUE_e under water-limited conditions. R_d for Brahmaputra basin (*Basin Id 2b*, the basin with highest WUE_m) was slightly above 1, indicating the resilient characteristics of ecosystems in the basin. *Basin Id. 20*, which had low WUE_m (= 0.348 gC m^{-2} mm^{-1}) and located in arid and semi-arid drought affected regions of Rajasthan and Gujarat, was also resilient (R_d = 1.189). The ecosystems in arid regions are habituated to the water-limited conditions due to frequent droughts and hence, have an inherent resilience to such

TABLE 1 Ecosystem resilience analysis at the basin scale

Basin ID	WUE_m	Driest year	Mean SPI6 for driest year	Mean SPEI6 for driest year	Precipitation in the driest year (mm)	WUE_d	$R_d = \frac{WUE_d}{WUE_m}$	Resilient ($R_d \geq 1$)
1[a]	0.802	2002	−0.89	−1.20	466	1.055	1.315	True
2a	0.729	2009	−2.09	−1.02	812	0.67	0.92	False
2b[a]	1.111	2001	−1.32	−0.71	1982	1.115	1.004	True
2c	0.895	2006	−1.25	−0.73	1741	0.845	0.944	False
3	0.387	2009	−1.39	−1.37	861	0.277	0.716	False
4	0.438	2003	−1.37	−1.09	554	0.373	0.851	False
5	0.643	2002	−2.79	−1.69	488	0.635	0.988	False
6	0.533	2010	−1.73	−0.90	891	0.37	0.695	False
7	0.586	2010	−1.51	−1.50	1081	0.449	0.766	False
8	0.556	2000	−1.3	−0.59	888	0.493	0.887	False
9[a]	0.631	2014	−0.87	−0.75	490	0.715	1.134	True
10	0.249	2000	−0.88	−0.92	454	0.147	0.592	False
11	0.288	2002	−1.15	−1.18	382	0.283	0.982	False
12	0.366	2000	−0.99	−0.47	681	0.236	0.643	False
13	0.325	2000	−0.55	−0.32	563	0.203	0.624	False
14	0.507	2002	−1.2	−0.59	2220	0.487	0.961	False
15	0.587	2002	−0.47	−0.98	911	0.533	0.909	False
16	0.508	2002	−0.96	−0.59	697	0.438	0.862	False
17[a]	0.633	2014	−0.7	−0.98	582	0.792	1.25	True
18[a]	0.799	2002	−2.2	−1.52	464	0.844	1.056	True
19	0.724	2003	−2.4	−1.94	312	0.7	0.968	False
20[a]	0.348	2002	−0.92	−1.08	232	0.414	1.189	True

SPI6 and SPEI6 represent the 6-month standardized precipitation index and standardized precipitation evapotranspiration index.
[a]Represents the resilient ($WUE_d \geq WUE_m$) basins.

conditions. In addition, three basins along the coastal south India (*Basins Id's 9, 17 and 18*) were also found resilient. Seven basins including the Ganga basin (*Basin Id. 2a*, the largest and most populous basin) were found slightly nonresilient ($0.9 \leq R_d < 1$). The basins along the Western Ghats (*Basin Id. 14*), which have generally water surplus because of high annual rainfall, failed to maintain their WUE_m during the driest year. Three basins (*Basin Id's 4, 8, and 16*) were found moderately nonresilient ($0.8 \leq R_d < 0.9$). Ecosystems in the central and eastern regions of the country were least resilient to dry conditions as R_d was less than 0.8 for all the basins in the region. Among all basins, the Mahi basin (*Basin Id. 10*) had the highest degree of nonresilience (R_d = 0.592).

3.5 | Ecosystem resilience analysis at land cover scale

The ecosystem resilience analysis for the major land cover types was carried out to understand the factors controlling the ecosystem resilience at the basin scale. Table 2 shows the ecosystem resilience analysis at land cover scale. Only evergreen forests (*ENF* and *EBF*) were found resilient (i.e., $R_d \geq 1$) which partially explains the resilience of forest-dominated Brahmaputra basins (*Basin Id 2b*). Deciduous broadleaf forest (DBF), which had least WUE_m among forest covers, was the least resilient (R_d = 0.70). The WUE_e for grasslands (GR), the most sensitive biome to water availability (Ponce Campos et al., 2013), decreased slightly for the driest year (R_d = 0.98). Croplands (CR and CNV), the largest land cover in India, had similar behavior as GR under dry conditions. The ecosystem resilience of Ganga basin (*Basin Id 2a*) is consistent with the presence of large croplands.

3.6 | Ecosystem resilience analysis at climate type scale

Ecosystem resilience analysis of different climate types indicated that only three climate types, namely, *Csa*, *Cwb*, and *ET*, were resilient to hydroclimatic disturbances during the study duration (Table 3). *Csa* was found the most resilient (R_d = 1.060). The ecosystem productivity of *BWh* climate type was most affected by the dry conditions (R_d = 0.627).

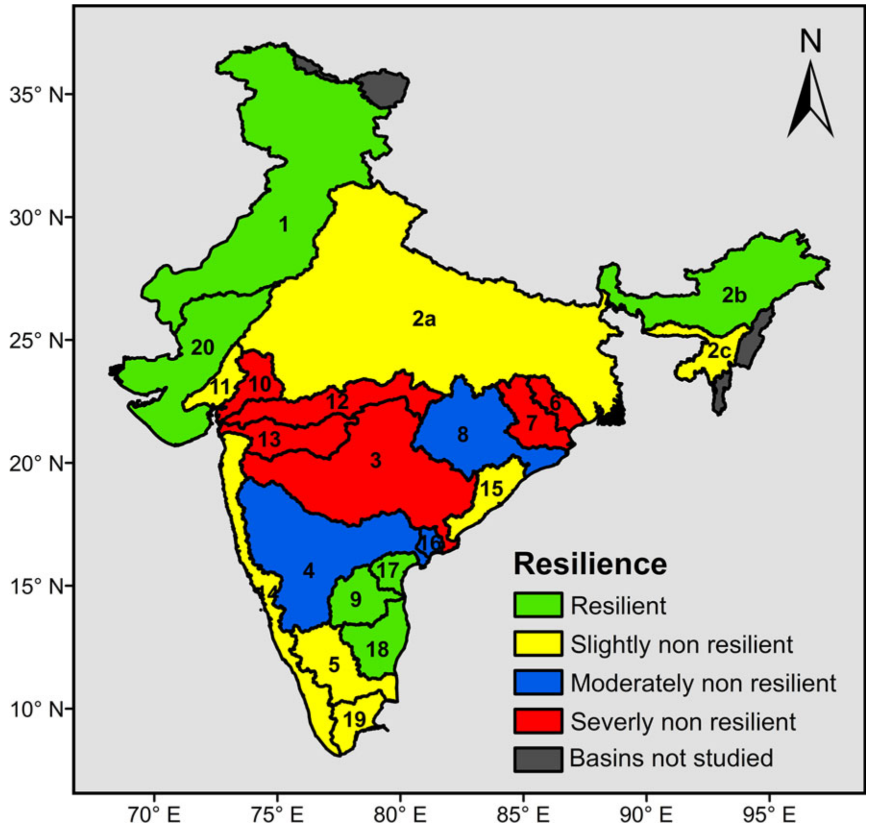

FIGURE 4 Ecosystem resilience of different river basins in India

TABLE 2 Ecosystem resilience analysis at land cover scale

Land cover type	WUE_m	Driest year	Precipitation in the driest year (mm)	WUE_d	$R_d = \frac{WUE_d}{WUE_m}$	Resilient ($R_d \geq 1$)
Evergreen Needleleaf Forest (ENF)[a]	0.959	2001	1612	0.990	1.03	True
Evergreen Broadleaf Forest (EBF)[a]	0.948	2012	1934	0.951	1.00	True
Deciduous Broadleaf Forest (DBF)	0.416	2002	983	0.290	0.70	False
Mixed Forests (MF)	1.087	2012	1440	1.034	0.95	False
Grasslands (GR)	0.488	2009	1030	0.478	0.98	False
Croplands (CR)	0.619	2002	743	0.609	0.98	False
Cropland/Natural Vegetation Mosaic (CNV)	0.689	2002	1008	0.671	0.97	False

[a]Represents the resilient ($WUE_d \geq WUE_m$) land covers.

4 | DISCUSSION

4.1 | WUE_e at different scales

Water is the most important limiting factor for primary productivity in India (Running et al., 2004). Addition of water due to elevated precipitation will simulate the primary productivity more than the ET, leading to the increase in WUE_e. Figure 1a,b shows that Brahmaputra basin (*Basin Id 2b*) had the highest WUE_m (= 1.111 gC m^{-2} mm^{-1}), which can mainly be attributed to the presence of forests in the basin (Figure 2a), as forest classes had higher WUE_m compared to other land cover types (Figure 2b). Among all river basins, northeastern basins have the largest forest cover. EBF and MF, respectively, covers about 24.45% and 21.82% of area in the Brahmaputra basin, with total forest cover about 50% of the basin area. Similar to Brahmaputra basin, neighboring Barak and other basins (*Basin Id 2c*) also have large forest cover about 60.81% of the basin area and, therefore, have higher WUE_m. On the other hand, Mahi basin (*Basin Id 10*) has

TABLE 3 Ecosystem resilience analysis at Koppen-Geiger climate type scale

Climate Type	Percent Area (%)	WUE_m	Driest year	Precipitation in the driest year (mm)	WUE_d	$R_d = \frac{WUE_d}{WUE_m}$	Resilient ($R_d \geq 1$)
Am	2.99	0.535	2002	1930.38	0.513	0.958	False
As	5.51	0.400	2000	787.19	0.261	0.653	False
Aw	25.88	0.504	2002	892.21	0.425	0.844	False
BWh	6.48	0.175	2002	95.21	0.110	0.627	False
BSh	21.45	0.475	2002	440.07	0.429	0.903	False
Csa[a]	6.63	0.476	2007	692.14	0.505	1.060	True
Cwa	19.32	1.055	2009	1257.54	1.041	0.987	False
Cwb[a]	3.16	1.009	2001	1515.10	1.027	1.018	True
ET[a]	3.29	0.242	2014	545.71	0.257	1.060	True

[a]Represents the resilient ($WUE_d \geq WUE_m$) climate types.

the least WUE_m (= 0.249 gC m^{-2} mm^{-1}) due to the absence of forest area (<1%), where cropland covers about 83% of basin area (Figure 2a). The basin had least WUE_m due to the low productivity and high ratio of evaporation to ET associated with sparse vegetation. It should be noted that Brahmaputra basin has one of the highest mean annual precipitation (MAP), whereas the Mahi basin has much smaller MAP (Figure 2b), which shows the dependence of WUE_e on precipitation. In contrast to the good correlation between WUE_m and MAP for different basins, the west flowing rivers South of Tapi Basin (*Basin Id 14*) had the highest MAP but lesser WUE_m (= 0.507 gC m^{-2} mm^{-1}). *Basin Id 18* had relatively higher WUE_m (= 0.799 gC m^{-2} mm^{-1}) compared to other basins in southern regions due to the large presence of CNV. The moderate WUE_m (= 0.802 gC m^{-2} mm^{-1}) of Indus basin (*Basin Id 1*) was due to the presence of forests in lower Himalayan regions.

Due to different patterns of eco-hydrological process among different vegetation types, the land cover type was one of the major factors controlling the WUE_e at basin scale. In addition to vegetation types, the hydroclimatic conditions also control the ecological and hydrological process such as evapotranspiration, plant respiration, etc. For Indian region, we found that *Cwa* and *Cwb* climate types had the highest WUE_m (Figure 3b). These climate types are mainly present in the Brahmaputra basin (*Basin Id 2b*, Figure 3a), which had the highest WUE_m. One the other hand, the arid climate types (i.e., *BWh* and *BSh*) had least WUE_m, which was consistent with the lesser WUE_m of basins (*Basin Id's 10, 11, 12, 13, and 20*) in the western regions.

4.2 | Ecosystem resilience to hydroclimatic disturbances at different scales

The primary productivity of the ecosystems is affected differently by the hydroclimatic conditions at different scales because the response of the ecosystems at different scales is controlled by different ecohydrological processes. For example, in arid regions, the productivity is controlled by the water availability, whereas in mountain regions solar radiation is the controlling factor. The resilience of an ecosystem to the disturbance represents the cross-biome capability to tolerate the disturbed conditions (Ponce Campos et al., 2013). For Indian conditions, the major climatic control on the vegetation productivity is the water availability or precipitation (Running et al., 2004). A decrease (increase) in water availability to the vegetation will result in lower (higher) primary productivity. We evaluated the ecosystem resilience in terms of the capability of an ecosystem to maintain its productivity during the hydroclimatic disturbance (i.e., water-limited conditions). Our results show that only 6 (of 22) river basins were able to sustain their primary productivity by increasing the WUE_e under driest year (Figure 4). As the ecosystem response to the hydroclimatic changes is driven by the dominant species, we related the ecosystem resilience of a basin to the land cover types and climate types present in the basin. The land-cover-scale ecosystem resilience analysis indicated that only two forest classes (*ENF* and *EBF*) were resilient during the study duration (Table 2). The presence of these biomes in Brahmaputra basin could be the reason for the resilient characteristics of the basin. In addition, Brahmaputra basin has *Cwa* and *Cwb* climate types, which were found resilient (Table 3). A dynamic vegetation modeling-based study on Indian forests also found the northeastern forests resilient to climatic changes (Chaturvedi et al., 2011). The least resilient basins include *Basin Id's 3, 6, 7, 10, 12, and 13*, which are mainly located in the central India. CR and Woody Savannas (WS) are the major land cover types in these regions; whereas *Aw*, *As*, and *BSh* are the dominant climate types. Our results showed that these land cover or climate types were not resilient, which had resulted into nonresilient characteristics of the central India. Forests in some parts of Western Ghats and central India were found more vulnerable (least resilient) to climate change (Chaturvedi et al., 2011), which was consistent with our results. Ganga basin, the most populous and agriculturally important basin, (*Basin Id 2a*) was also found slightly nonresilient (R_d = 0.920). CR is the most dominant land cover type in the basin, and *Csa*, *Aw*, and *Cwa* are the major climate types. Although *Csa* was found resilient, but the contribution from other climate types have resulted in overall nonresilient characteristics of the basin. The anthropogenic factors such as population growth, deforestation, agricultural activities, urbanization, and construction activities have deteriorated the ecology of the basin (Sarkar, Bhattacharya, & Bhattacharya, 2003), which could be the possible reason behind the nonresilient characteristics of the basin. *Aw* climate type, the most dominant climate in the eastern and southern regions, was found moderately nonresilient (R_d = 0.844), which was also consistent with basins falling in these regions except for *Basin Id's 9, 17, and 18*. *As* climate type, mainly limited to the central parts, was found severely nonresilient (R_d = 0.653) and was consistent with basins in central parts (*Basin Id's 3, 12, and 13*). The nonresilient characteristics of the ecosystem in these basins were consistent with the higher vulnerability of forests in the region to climate change (Chaturvedi et al., 2011). Ecosystems in arid climate were found nonresilient, which was consistent with Krishna basin (*Basin Id 4*). On the other hand, *Basin Id 20* was found resilient which was inconsistent with the presence of arid climates. Although land cover and climate type were related to the ecosystem resilience of some basins, but the ecosystem response in other basins cannot be completely related to these two factors due to substantial eco-hydrological variations within the basins. This highlights that there is a need to further investigate the eco-hydrological processes that govern the complex climate–soil–plant interactions.

4.3 | Implications for climate change

The results of our study facilitate understanding of how ecosystems in different regions of the country respond to hydroclimatic disturbances. Under the scenarios of increasing trend in drought severity and frequency during the recent decades (Mallya et al., 2015; Mishra, Aadhar, Akarsh, Pai, & Kumar, 2016) and projected future possible reductions in monsoon-related rainfall in the country (Prabhakar & Shaw, 2008), ecosystems in India will face many hydroclimatic disturbances such as droughts. The nonresilient characteristics of most river basins suggested that the NPP would decrease under such conditions in the future. The results of this study are compelling as it highlights that ecosystems in most of the basins are not resilient to hydroclimatic disturbances as anticipated for future through increasing trend of droughts in India (Mallya et al., 2015). The inability of ecosystems at different scales to tolerate the water-limited conditions may pose a serious challenge in terms of carbon sequestration, crop production, and food security. This study, to our knowledge, is the first to relate WUE_e with ecosystem resilience in India. Our results also provide the knowledge about the hotspots for the ecosystem management and climate policy making.

ORCID

Ashutosh Sharma http://orcid.org/0000-0003-2613-2821
Manish Kumar Goyal http://orcid.org/0000-0001-9777-6128

REFERENCES

Anav, A., Friedlingstein, P., Beer, C., Ciais, P., Harper, A., Jones, C., ... Zhao, M. (2015). Spatiotemporal patterns of terrestrial gross primary production: A review. *Reviews of Geophysics*, *53*, 785–818.

Asoka, A., Gleeson, T., Wada, Y., & Mishra, V. (2017). Relative contribution of monsoon precipitation and pumping to changes in groundwater storage in India. *Nature Geoscience*, *10*, 109–117.

Breshears, D. D., Cobb, N. S., Rich, P. M., Price, K. P., Allen, C. D., Balice, R. G., ... Meyer, C. W. (2005). Regional vegetation die-off in response to global-change-type drought. *Proceedings of the National Academy of Sciences of the United States of America*, *102*, 15144–15148.

Broxton, P. D., Zeng, X., Sulla-Menashe, D., & Troch, P. A. (2014). A global land cover climatology using MODIS data. *Journal of Applied Meteorology and Climatology*, *53*, 1593–1605.

Cao, M. K., & Woodward, F. I. (1998). Dynamic responses of terrestrial ecosystem carbon cycling to global climate change. *Nature*, *393*, 249–252.

Chaturvedi, R. K., Gopalakrishnan, R., Jayaraman, M., Bala, G., Joshi, N. V., Sukumar, R., & Ravindranath, N. H. (2011). Impact of climate change on Indian forests: A dynamic vegetation modeling approach. *Mitigation and Adaptation Strategies for Global Change*, *16*, 119–142.

Ciais, P., Reichstein, M., Viovy, N., Granier, A., Ogée, J., Allard, V., ... Valentini, R. (2005). Europe-wide reduction in primary productivity caused by the heat and drought in 2003. *Nature*, *437*, 529–533.

Ciais, P., Tans, P. P., Trolier, M., White, J. W. C., & Francey, R. J. (1995). A large northern hemisphere terrestrial CO2 sink indicated by the 13C/12C ratio of atmospheric CO2. *Science*, *269*, 1098–1102.

Dai, A. (2011). Drought under global warming: A review. *Wiley Interdisciplinary Reviews: Climate Change*, *2*, 45–65.

Dai, A. (2013). Increasing drought under global warming in observations and models. *Nature Climate Change*, *3*, 52–58.

Dale, V. H., Joyce, L. A., McNulty, S., & Neilson, R. P. (2000). The interplay between climate change, forests, and disturbances. *Science of the Total Environment*, *262*, 201–204.

Elmqvist, T., Folke, C., Nystrom, M., Peterson, G., Bengtsson, J., Walker, B., & Norberg, J. (2003). Response diversity, ecosystem change, and resilience. *Frontiers in Ecology and the Environment*, *1*, 488–494.

Huang, M., Piao, S., Sun, Y., Ciais, P., Cheng, L., Mao, J., ... Wang, Y. (2015). Change in terrestrial ecosystem water-use efficiency over the last three decades. *Global Change Biology*, *21*, 2366–2378.

Huang, M., Piao, S., Zeng, Z., Peng, S., Ciais, P., Cheng, L., ... Wang, Y. (2016). Seasonal responses of terrestrial ecosystem water-use efficiency to climate change. *Global Change Biology*, *22*, 2165–2177.

India-WRIS (2014). *Watershed Atlas of India*. New Delhi: Central Water Commision and National Remote Sensing Center ISRO.

Jones, H. (2004). What is water use efficiency? In M. Bacon (Ed.), *Water use efficiency in plant biology* (pp. 27–41). Oxford: Blackwell Publishing Ltd.

Karl, T. R., & Trenberth, K. E. (2014). Modern global climate change. *Science*, *302*, 1719–1723.

Keenan, T. F., Hollinger, D. Y., Bohrer, G., Dragoni, D., Munger, J. W., Schmid, H. P., & Richardson, A. D. (2013). Increase in forest water-use efficiency as atmospheric carbon dioxide concentrations rise. *Nature*, *499*, 324–327.

Kottek, M., Grieser, J., Beck, C., Rudolf, B., & Rubel, F. (2006). World map of the Köppen-Geiger climate classification updated. *Meteorologische Zeitschrift*, *15*, 259–263.

Mallya, G., Mishra, V., Niyogi, D., Tripathi, S., & Govindaraju, R. S. (2015). Trends and variability of droughts over the Indian monsoon region. *Weather and Climate Extremes*, *12*, 43–68.

McKee, T. B., Doesken, N. J., & Kleist, J. (1993). The relationship of drought frequency and duration to time scales. In *Proceedings of the 8th conference on applied climatology*, Boston, USA, pp. 179–184.

Meehl, G. A., & Tebaldi, C. (2004). More frequent, and longer lasting heat waves in the 21st century. *Science*, *305*, 994–997.

Mishra, V., Aadhar, S., Akarsh, A., Pai, S., & Kumar, R. (2016). On the frequency of the 2015 monsoon season drought in the Indo-Gangetic Plain. *Geophysical Research Letters*, *43*, 102–112.

Mu, Q., Heinsch, F. A., Zhao, M., & Running, S. W. (2007). Development of a global evapotranspiration algorithm based on MODIS and global meteorology data. *Remote Sensing of Environment*, *111*, 519–536.
Mu, Q., Zhao, M., & Running, S. W. (2011a). Evolution of hydrological and carbon cycles under a changing climate. *Hydrological Processes*, *25*, 4093–4102.
Mu, Q., Zhao, M., & Running, S. W. (2011b). Improvements to a MODIS global terrestrial evapotranspiration algorithm. *Remote Sensing of Environment*, *115*, 1781–1800.
Mu, Q., Zhao, M., & Running, S. W. (2013). *MODIS Global Terrestrial Evapotranspiration (ET) Product (MOD16A2/A3) - ATBD Collection 5* (66 pp.). Missoula, MT, USA: NASA.
Nemani, R. R., Keeling, C. D., Hashimoto, H., Jolly, W. M., Piper, S. C., Tucker, C. J., … Running, S. W. (2003). Climate-driven increases in global terrestrial net primary production from 1982 to 1999. *Science*, *300*, 1560–1563.
Niu, S., Xing, X., Zhang, Z., Xia, J., Zhou, X., Song, B., … Wan, S. (2011). Water-use efficiency in response to climate change: From leaf to ecosystem in a temperate steppe. *Global Change Biology*, *17*, 1073–1082.
Pachauri, R. K., & Meyer, L. A. (2014). *IPCC, 2014: Climate Change 2014: Synthesis Report. Contribution of Working Groups I, II and III to the Fifth Assessment Report of the Intergovernmental Panel on Climate Change* (pp. 1–151). Geneva: IPCC.
Pai, D. S., Sridhar, L., Rajeevan, M., Sreejith, O. P., Satbhai, N. S., & Mukhopadhyay, B. (2014). Development of a new high spatial resolution ($0.25° \times 0.25°$) long period (1901-2010) daily gridded rainfall data set over India and its comparison with existing data sets over the region. *Mausam*, *65*, 1–18.
Peel, M. C., Finlayson, B. L., & McMahon, T. A. (2007). Updated world map of the Koppen-Geiger climate classification. *Hydrology and Earth System Sciences*, *11*, 1633–1644.
Ponce Campos, G. E., Moran, M. S., Huete, A., Zhang, Y., Bresloff, C., Huxman, T. E., … Starks, P. J. (2013). Ecosystem resilience despite large-scale altered hydroclimatic conditions. *Nature*, *494*, 349–352.
Prabhakar, S. V. R. K., & Shaw, R. (2008). Climate change adaptation implications for drought risk mitigation: A perspective for India. *Climatic Change*, *88*, 113–130.
Roxburgh, S. H., Berry, S. L., Buckley, T. N., Barnes, B., & Roderick, M. L. (2005). What is NPP? Inconsistent accounting of respiratory fluxes in the definition of net primary production. *Functional Ecology*, *19*, 378–382.
Rubel, F., & Kottek, M. (2010). Observed and projected climate shifts 1901-2100 depicted by world maps of the Koppen-Geiger climate classification. *Meteorologische Zeitschrift*, *19*, 135–141.
Running, S. W., Nemani, R. R., Heinsch, F. A., Zhao, M., Reeves, M., & Hashimoto, H. (2004). A continuous satellite-derived measure of global terrestrial primary production. *BioScience*, *54*, 547–560.
Sarkar, S. K., Bhattacharya, A., & Bhattacharya, B. (2003). The river Ganga of northern India: An appraisal of its geomorphic and ecological changes. *Water Science and Technology*, *48*, 121–128.
Song, Q.-H., Fei, X.-H., Zhang, Y.-P., Sha, L.-Q., Liu, Y.-T., Zhou, W.-J., … Liu, Y.-H. (2017). Water use efficiency in a primary subtropical evergreen forest in Southwest China. *Scientific Reports*, *7*, 43031.
Sun, Y., Piao, S., Huang, M., Ciais, P., Zeng, Z., Cheng, L., … Zeng, H. (2016). Global patterns and climate drivers of water-use efficiency in terrestrial ecosystems deduced from satellite-based datasets and carbon cycle models. *Global Ecology and Biogeography*, *25*, 311–323.
Tang, X., Li, H., Desai, A. R., Nagy, Z., Luo, J., Kolb, T. E., … Ammann, C. (2014). How is water-use efficiency of terrestrial ecosystems distributed and changing on Earth? *Scientific Reports*, *4*, 7483.
Thomey, M. L., Collins, S. L., Vargas, R., Johnson, J. E., Brown, R. F., Natvig, D. O., & Friggens, M. T. (2011). Effect of precipitation variability on net primary production and soil respiration in a Chihuahuan Desert grassland. *Global Change Biology*, *17*, 1505–1515.
Turner, D. P., Ritts, W. D., Cohen, W. B., Gower, S. T., Running, S. W., Zhao, M., … Ahl, D. E. (2006). Evaluation of MODIS NPP and GPP products across multiple biomes. *Remote Sensing of Environment*, *102*, 282–292.
Vicente-Serrano, S. M., Beguería, S., & López-Moreno, J. I. (2010). A multiscalar drought index sensitive to global warming: The standardized precipitation evapotranspiration index. *Journal of Climate*, *23*, 1696–1718.
Walker, B., Holling, C. S., Carpenter, S. R., & Kinzig, A. (2004). Resilience, adaptability and transformability in social – ecological systems. *Ecology and Society*, *9*, 5.
Wheeler, T., & Von Braun, J. (2013). Climate change impacts on global food security. *Science*, *341*, 508–513.
Xia, L., Wang, F., Mu, X., Jin, K., & Sun, W. (2015). Water use efficiency of net primary production in global terrestrial ecosystems. *Journal of Earth System Science*, *124*, 921–931.
Xu, C., Liu, H., Anenkhonov, O. A., Korolyuk, A. Y., Sandanov, D. V., Balsanova, L. D., … Wu, X. (2017). Long-term forest resilience to climate change indicated by mortality, regeneration, and growth in semiarid southern Siberia. *Global Change Biology*, *23*, 2370–2382.
Xue, B.-L., Guo, Q., Otto, A., Xiao, J., & Tao, S. (2015). Global patterns, trends, and drivers of water use efficiency from 2000 to 2013. *Ecosphere*, *6*, 1–18.
Yang, Y., Guan, H., Batelaan, O., McVicar, T. R., Long, D., Piao, S., … Simmons, C. T. (2016). Contrasting responses of water use efficiency to drought across global terrestrial ecosystems. *Scientific Reports*, *6*, 23284.
Yu, G., Chen, Z., Piao, S., Peng, C., Ciais, P., Wang, Q., … Zhu, X. (2014). High carbon dioxide uptake by subtropical forest ecosystems in the East Asian monsoon region. *Proceedings of the National Academy of Sciences*, *111*, 4910–4915.
Zhang, X., Obringer, R., Wei, C., Chen, N., & Niyogi, D. (2017). Droughts in India from 1981 to 2013 and implications to wheat production. *Scientific Reports*, *7*, 44552.
Zhao, M., Heinsch, F. A., Nemani, R. R., & Running, S. W. (2005). Improvements of the MODIS terrestrial gross and net primary production global data set. *Remote Sensing of Environment*, *95*, 164–176.
Zhao, M., & Running, S. W. (2010). Drought-induced reduction in global terrestrial net primary production from 2000 through 2009. *Science*, *329*, 940–943.
Zhao, M., Running, S. W., & Nemani, R. R. (2006). Sensitivity of Moderate Resolution Imaging Spectroradiometer (MODIS) terrestrial primary production to the accuracy of meteorological reanalyses. *Journal of Geophysical Research: Biogeosciences*, *111*, 1–13.

SUPPORTING INFORMATION

Additional Supporting Information may be found online in the supporting information tab for this article.

How to cite this article: Sharma A, Goyal MK. Assessment of ecosystem resilience to hydroclimatic disturbances in India. *Glob Change Biol*. 2017;00:1–10. https://doi.org/10.1111/gcb.13874